



# Abiotic degradation and environmental toxicity of ibuprofen: Roles of mineral particles and solar radiation

Gayan Rubasinghege<sup>a, \*</sup>, Rubi Gurung<sup>a</sup>, Hom Rijal<sup>a</sup>, Sabino Maldonado-Torres<sup>a</sup>, Andrew Chan<sup>a</sup>, Shishir Acharya<sup>b</sup>, Snezna Rogelj<sup>b</sup>, Menake Piyasena<sup>a</sup>

<sup>a</sup> Department of Chemistry, New Mexico Tech, Socorro, NM 87801, United States

<sup>b</sup> Department of Biology, New Mexico Tech, Socorro, NM 87801, United States

## ARTICLE INFO

### Article history:

Received 20 July 2017

Received in revised form

30 November 2017

Accepted 9 December 2017

Available online 11 December 2017

### Keywords:

Pharmaceuticals

Photo-enhanced toxicology

Abiotic transformation

Personal care products

Photo degradation

Secondary products

## ABSTRACT

The growing medical and personal needs of human populations have escalated release of pharmaceuticals and personal care products into our natural environment. This work investigates abiotic degradation pathways of a particular PPCP, ibuprofen, in the presence of a major mineral component of soil (kaolinite clay), as well as the health effects of the primary compound and its degradation products. Results from these studies showed that the rate and extent of ibuprofen degradation is greatly influenced by the presence of clay particles and solar radiation. In the absence of solar radiation, the dominant reaction mechanism was observed to be the adsorption of ibuprofen onto clay surface where surface silanol groups play a key role. In contrast, under solar radiation and in the presence of clay particles, ibuprofen breaks down to several fractions. The decay rates were at least 6-fold higher for irradiated samples compared to those of dark conditions. Toxicity of primary ibuprofen and its secondary residues were tested on three microorganisms: *Bacillus megaterium*, *Pseudoaltermonas atlantica*; and algae from the *Chlorella* genus. The results from the biological assays show that primary PPCP is more toxic than the mixture of secondary products. Overall, however, biological assays carried out using only 4-acetylbenzoic acid, the most abundant secondary product, show a higher toxic effect on algae compared to its parent compound.

© 2017 Elsevier Ltd. All rights reserved.

## 1. Introduction

Pharmaceuticals and personal care products (PPCPs) are, in general, any product used for personal health or cosmetic reasons or used by agribusiness to enhance growth or health of livestock (Boxall et al., 2012). Majority of the PPCPs emerge in the environment via medication residues that pass out of the body, used or expired medications placed in the trash, or personal care products washed down the shower drain (Overturf et al., 2015). Hundreds of individual PPCPs have been detected at parts-per-billion and parts-per-trillion concentrations in wastewater and surface water (Deo, 2014). In recent studies, active pharmaceutical compounds (PhACs), i.e. clofibrac acid, ibuprofen, diclofenac, and bisphenol A, have been identified at concentrations up to 1 g/L in affluent and effluent waters (Blair et al., 2013). These studies also highlight the occurrence of PhACs in drinking water at concentrations of ng/L

(Khan and Nicell, 2015). Many of these compounds are not removed by wastewater treatment; this has become a particular concern if drinking-water sources include a substantial fraction of treated wastewater effluent (Kolpin et al., 2002).

Pharmaceuticals, as well as several chemicals used in personal care products, are biologically active compounds which are designed to interact with particular biological pathways in target humans and animals at prescribed doses. Consequently, some PPCPs are well-known endocrine disruptors and cause adverse effects in the reproductive system of humans and wildlife (Kortenkamp et al., 2009; Overturf et al., 2015). In the environment, some PPCPs are quickly metabolized or degraded quickly while others persist and may also be mobile. Xu et al. and others have reported limited breakdown of selected PPCPs in the presence of agricultural soil and have attributed the differences in degradation to the differences in the indigenous microbial population of the soil (Xu et al., 2009). However, Ternes and co-workers have shown that biodegradation pathways of PPCPs appear to be slow and persistent against bacterial degradation (Ternes et al., 2004). Yet, secondary products of PPCPs, resulting from environmental processes, have

\* Corresponding author.

E-mail address: [gayan.rubasinghege@nmt.edu](mailto:gayan.rubasinghege@nmt.edu) (G. Rubasinghege).

been found in water and soil (Li, 2014). In a recent study, Jacobs et al. highlights that breakdown of ibuprofen is 6-fold faster in the presence of organic matter, e.g.: fulvic acid (Jacobs et al., 2011). However, little is known about exact molecular level processes and the influence of environmental conditions on above degradation pathways. Perhaps even more importantly, the toxicity of the secondary residues is unknown. Thus, the current work attempts to fill this knowledge gap by a detail study to gain molecular level insights of fate, transformation and long-term health effects of PPCPs and their secondary residues.

PPCPs released to the environment are in constant interaction with soil particles, a complex mixture of metals, metal oxides and clay particles. Thus, soil particles provide a reactive surface for heterogeneous chemical and photochemical reactions to occur. The current study focuses on abiotic degradation pathways of a particular PPCP, ibuprofen, in the presence of a major mineral component of soil, kaolinite clay. Ibuprofen was selected as a proxy for PPCPs due to its high environmental abundance, inherent toxicity and structural features similar to many PPCP compounds. Chemical and photochemical reactions of ibuprofen were also studied under light and dark conditions so as to simulate and differentiate between daytime and nighttime processing of PPCPs. The results of this study, for the first time, propose a detailed reaction mechanism for the abiotic degradation of ibuprofen, starting from surface adsorption to the formation of particular secondary products. Further, the current work evaluates the toxicity of ibuprofen and its degraded products on three microorganisms. Thus, we provide a detailed report on potential toxic effects of degraded secondary residues - a heretofore-unexamined process. The information will be used to interpret field observations of PPCP residues and their toxic effects on aquatic life and human health as they are transformed under various environmental conditions. This work therefore contributes to our understanding of pharmaceutical mobilization in water bodies.

## 2. Materials and methods

### 2.1. Chemicals and reagents

Ibuprofen ( $\geq 99.5\%$ , Sigma-Aldrich) and 4-acetylbenzoic acid ( $\geq 98\%$ , Sigma-Aldrich) were used as reference material. During solution preparation, double DI Milli-Q water (Res > 18.2 M $\Omega$ , Millipore Advance A10) was used. Kaolinite, KGa-1b, from the Source Clay Repository in Washington County, Georgia, was used as a proxy soil mineral. In toxicological studies, dimethyl sulfoxide (certified ACS, Fisher Scientific) was used to prepare standard solution. Phenylarsine oxide ( $\geq 97\%$ , Sigma-Aldrich) was used as the “complete kill” control. Nutrient broth (BD Difco™) and Marine broth (BD Difco™) served the bacterial growth media. Algal cells were grown using Alga-Gro® Freshwater medium (Carolina). MTT reagent (3-(4,5-Dimethylthiazol-2-yl)-2,5-Diphenyltetrazolium Bromide; Fisher) was used to prepare 5 mg/mL stock solution in PBS and added to a final concentration of 0.5 mg/mL.

### 2.2. Particle characterization

Clay (kaolinite) was characterized using powder X-ray diffraction (XRD) performed on a Bruker D-5000 diffractometer with a Cu K $\alpha$  source. FTIR spectra of kaolinite particles were obtained using a Thermo.

Scientific IS50 spectrophotometer equipped with a Ge internal reflective element (IRE). Surface areas were determined from a seven-point N $_2$ -BET isotherm using a Quantachrome Autosorb1 surface area analyzer. Particle dimensions were obtained from single particle analysis with Scanning Electron Microscopy (SEM).

Particle size was determined from the analysis of approximately 300 particles.

### 2.3. Degradation studies

#### 2.3.1. Batch reactor studies

The experiments were carried out in a custom-built glass reactor using 10 mM ibuprofen solutions. Given the low sensitivity of current toxicological assays, high initial concentrations of ibuprofen were used. These experiments were conducted in the absence and the presence of solar simulator (150 W xenon lamp, New Port) with an Air Mass 0 filter. The temperature was kept constant through use of a water jacket. The particle loading was maintained 0.2 g/L of kaolinite in solutions of 10 mM ibuprofen. pH of the ibuprofen solution increased from 3.7 to 4.5 upon addition of kaolinite particles. Over time, samples were periodically removed from the reactor using a disposable syringe that was connected to 12 cm of Teflon tubing. Aliquots (1 mL) were collected into HPLC vials after passing through a 0.2  $\mu$ m PTFE filter (Expertek). Analysis of filtered extracts was performed by reverse phase HPLC (Agilent 1100). HPLC conditions are described in [Supporting Information](#).

#### 2.3.2. Liquid chromatography-mass spectroscopy (LC-MS)

Filtered samples collected at the end of batch reactor studies were analyzed using LC-MS to identify secondary products in the mixture. Here, the degraded solutions were concentrated and then analyzed using nano-flow liquid chromatography (Thermo Fisher Ultimate 3000RLS Nano) coupled with an Orbitrap Fusion Tribrid mass spectrometer (Thermo Fisher) that provided high resolution, accurate mass measurement and multiple fragmentation mechanisms for molecular structural elucidation. Details of LC-MS experimental conditions are described in [Supporting Information](#).

### 2.4. Biological studies

#### 2.4.1. Experimental setup

Stock solutions of ibuprofen and 4-acetylbenzoic acid were prepared in DMSO at concentration of 100 mM. A 96 well-plate experimental setup is illustrated in [Supporting Information \(SI Fig. 1\)](#). Briefly, each of the wells was filled with 150  $\mu$ L of bacterial or algal cell suspension. 3.0  $\mu$ L of 100 mM ibuprofen stock solution was pipetted to the first well to attain the final drug concentration of 1 mM. 150  $\mu$ L was then transferred from the first well to the second well. This 1:2 serial dilution process was repeated until the lowest test concentration (15.6  $\mu$ M) was obtained. The effect of two solvents, water and DMSO, was also studied to evaluate any effect on the growth of organisms. Additionally, phenylarsine oxide (PAO) was used as a positive control, “complete-dead” or “complete-killed”, and was tested at final concentration of about 67  $\mu$ M. The well-plates containing *B. megaterium* and *P. atlantica* were incubated at 30 °C with gentle shaking. Alternately, the plate with *Chlorella* cells was placed on a rotary shaker (72 rpm) at room temperature underneath a 17 W fluorescent light on a 12 h light and dark cycle.

#### 2.4.2. Toxicological assays

Cell densities for *B. megaterium*, *P. atlantica* and *Chlorella* cells were monitored through OD measurements at 595 nm using Microplate Reader (Molecular Devices). Viability of bacterial cells was further measured using standard MTT assay. At 24 h, 30  $\mu$ L of 5 mg/mL of MTT reagent was added to each well of the 96 well-plate and incubated for 1 h at 30 °C. After the period of incubation, they were solubilized in 200  $\mu$ L of DMSO. OD measurements were taken at 490 nm. BD FACScalibur flow cytometer was used to assess the comparative toxic effects between ibuprofen and its secondary products on algal cell size, granularity/shape, and

autofluorescence. Algal samples were collected at 0, 24, and 48 h for flow cytometric analysis. The BD CellQuest Pro Software was used to collect the data while FCS Express 5 (De Novo software) was used for data analysis.

### 2.5. Statistical analysis

All dark and light experiments were conducted in triplicate with average measurements reported. Reported errors represent one standard deviation. Variations among different treatments, statistically significant at 95% confidence level, were identified using the paired *t*-test in MINITAB 17. Results were considered significant when *p*-value < .05.

## 3. Results and discussion

### 3.1. Characterization of kaolinite particles

The surface area of the clay mineral, kaolinite, is  $10.1 \pm 0.1 \text{ m}^2/\text{g}$ . SEM image of kaolinite clay sample is shown in Fig. 1A. It is apparent that the clays are highly irregular in shape. As shown in Fig. 1B, quartz, a mineral commonly noted to be an impurity, was not detected in the clay samples used in this study as determined

from the crystal structure library. ATR-FTIR spectroscopy can also provide insights into the bulk and surface properties of clay minerals. Fig. 1C displays the ATR-FTIR spectra of clay mineral after overnight drying at <5% RH. A magnified view of the spectral region from  $3550$  to  $3750 \text{ cm}^{-1}$  for kaolinite is also shown in Fig. 1C insert. These absorptions are assigned to the characteristic peaks due to the OH-stretching motion of interlayer hydroxyl groups in various positions within the clay structure (Schuttlefield et al., 2007). These interlayer hydroxyl groups are structurally important for kaolinite reactivity because they actively participate in surface adsorption or surface-catalyzed reactions (Schuttlefield et al., 2007). In Fig. 1C, the spectral region from  $800$  to  $1600 \text{ cm}^{-1}$  shows absorptions due to lattice vibrations such as the Si–O stretching motions.

### 3.2. Abiotic degradation of ibuprofen

Chemical and photochemical degradation of ibuprofen were investigated in the presence of kaolinite to simulate processing of PPCPs under various light dependent environmental conditions to yield secondary residues. Due to the lower sensitivity of established toxicological assays, the initial concentrations of IBP used in the current work are higher than the concentrations reported in previous environmental studies. Given the higher degradation rates of

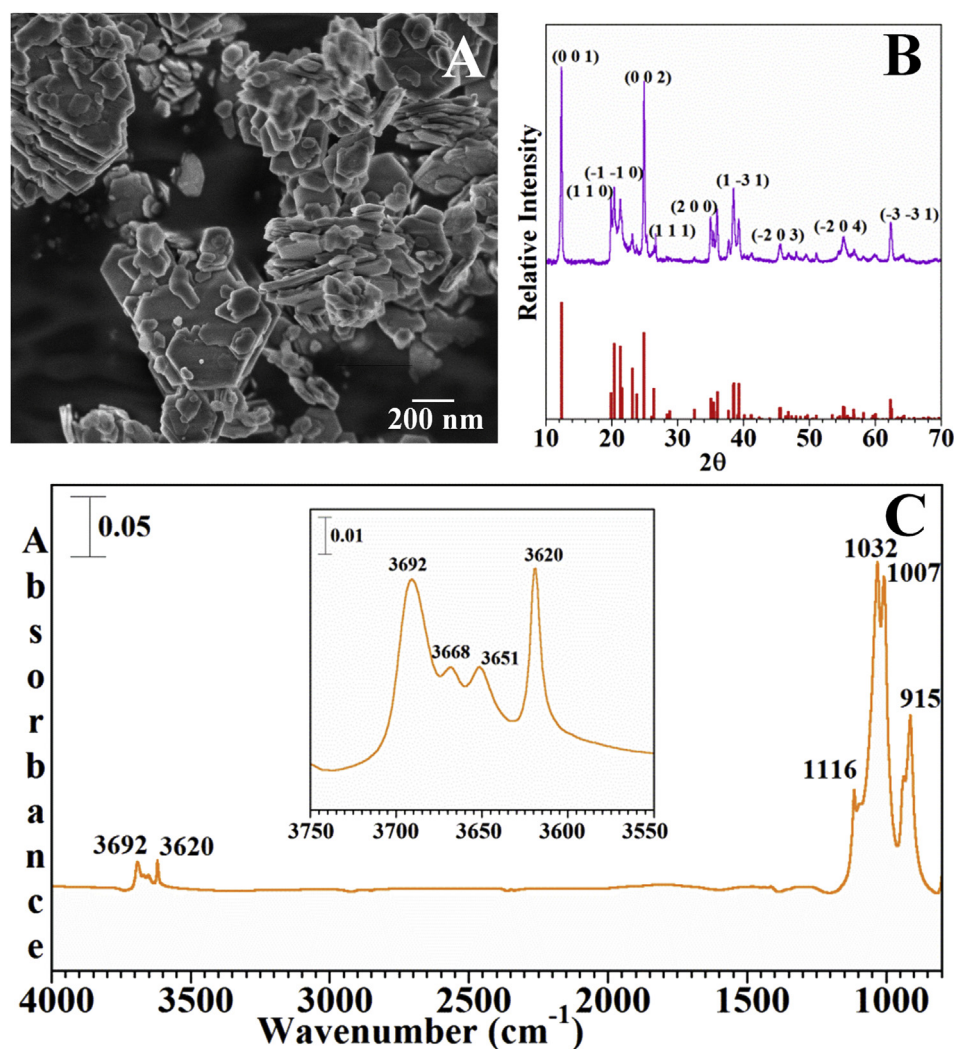


Fig. 1. Characterization of clay (Kaolinite) particles. A. Representative SEM image B. X-Ray Diffraction C. ATR-FTIR Spectrum of fresh clay sample under dry (%RH < 5) conditions. The spectral region from  $3550$  to  $3750 \text{ cm}^{-1}$  which was assigned to the characteristic bands associated with the OH-stretch of the inner-surface hydroxyl groups is expanded for clarity.

IBP, as shown below, it is expected that the amounts of IBP added to environment is even greater than that of reported, and thus the amount of secondary residues generated. It is also important to mention here that our preliminary studies, performed with lower IBP concentrations,  $\sim 100 \mu\text{M}$ , yielded degradation products similar to that found with starting 10 mM IBP concentration. (Data not shown). Moreover, these degraded products are expected to further accumulate in water bodies via biotic and abiotic mechanisms (Aceña et al., 2017). Thus, the implications discussed in this work, degradation and toxicological effects, are transferable to the environmentally-relevant conditions.

### 3.2.1. Role of clay particles

The data presented in Fig. 2 shows kinetics of ibuprofen degradation, determined from HPLC analysis of remaining ibuprofen in degraded samples. According to the comparison shown in Fig. 2A, the degradation rates of ibuprofen significantly varies based on experimental conditions. The degradation kinetics of ibuprofen, assuming pseudo-first order decay, is shown in Fig. 2B. The initial rates of degradation ( $r$ ), determined from linear regression ( $t < 50$  h), rate constants ( $k$ ), and correlation coefficients ( $R^2$ ) are given in Table 1. In both mass normalized and surface area normalized data, it can be clearly seen that the rate of ibuprofen decay in the presence of clay particles is faster and more extensive compared without clay. Under dark conditions, the initial rate of ibuprofen decay was  $0.24 (\pm 0.02) \times 10^{-4} \text{ M h}^{-1}$  whereas no decay was observed without clay (dark control). At the end of 240 h, the extent of ibuprofen removal was observed to be  $\sim 11\%$ . However, under dark conditions, no secondary product formation was observed in HPLC or LC-MS analysis. We therefore attribute the observed decay to the adsorption of ibuprofen onto clay particle surfaces. However, based on the measured surface area of kaolinite, 10 mM IBP is expected to yield a PPCP-to-solid ratio of  $\sim 30$  IBP molecules per  $\text{Å}^2$  of solid where the adsorption is limited by the number of available surface sites.

Khazri and co-workers have recently showed that natural clay, a mixture of smectite-kaolinite and quartz, can efficiently remove ibuprofen with a maximum adsorption capacity of  $37 \text{ mg g}^{-1}$  (Khazri et al., 2016). Based on their adsorption isotherm and IR data, authors also suggest that anionic or neutral PPCPs, i.e. ibuprofen, are adsorbed to the clay mineral surface via silanol groups at the sheet edges through interactional mechanisms involving van der Waals interaction. To gain additional molecular level insights into

the behavior of ibuprofen in the presence of clay particles, attenuated total reflection–Fourier transform infrared (ATR-FTIR) spectroscopy was used to investigate surface adsorption of ibuprofen on kaolinite. Details of solution phase ATR-FTIR experiments are provided in Supporting Information.

Fig. 3A shows several ATR-FTIR spectra for ibuprofen adsorption on kaolinite as a function of time. For comparison, a solution-phase spectrum of ibuprofen in the absence of kaolinite is also shown (top spectrum). It is important to highlight that, based on the  $\text{pK}_a$  of ibuprofen (5.2) and measured pH of the medium (4.5), major fraction of ibuprofen,  $\sim 90\%$ , exist in its molecular form. As a free molecule, ibuprofen showed several characteristic peaks including the peak at  $1719 \text{ cm}^{-1}$  for the C=O stretching mode of the –COOH group. The absorption bands at  $1462$  and  $1520 \text{ cm}^{-1}$  are assigned to the quaternary carbon atom (Madiéh et al., 2007). The ATR-FTIR surface spectra provide information on surface speciation. The most prominent difference between the solution spectrum and surface adsorbed spectra is the bathochromic shift of above described vibrational modes of ibuprofen and the appearance of a new peak at  $1240 \text{ cm}^{-1}$ . The C=O stretching mode is shifted by  $22 \text{ cm}^{-1}$  while the vibrational bands of quaternary carbon atom is shifted by  $\sim 90 \text{ cm}^{-1}$ . Similar chemical shifts have been observed in previous studies on adsorption of ibuprofen and other organic compounds on clays and aluminosilicates (Madiéh et al., 2007; Siampiringue et al., 2014). These vibrational shifts evidence the interactions between –COOH group of ibuprofen and silanol groups on clay surface during the formation of adsorption complexes of ibuprofen on clay particles.

In a recent work, Kamarudin et al. highlight that the interaction with silanol groups and –COOH group occur by two different pathways (Kamarudin et al., 2015). One pathway is via hydrogen bonding of silanol groups with the hydroxyl group of ibuprofen while the other is through ligand-exchange adsorption. The former pathway is favored due to the lower demand of activation energy and yields monodentate complexes (Kamarudin et al., 2015). The interactions via ligand-exchange can yield either monodentate or bidentate modes of coordination. The new peak at  $1240 \text{ cm}^{-1}$  can be attributed to (–O–C–O–) stretching of carboxylic acid group indicating the formation of bidentate complexes on the clay surface. These different modes of coordination are illustrated in Fig. 3B. Based on an adsorption mechanism proposed by Teresa and co-workers, benzylic carbon of the isobutyl residue may also interact with Brønsted acid sites (Blasco, 2010).

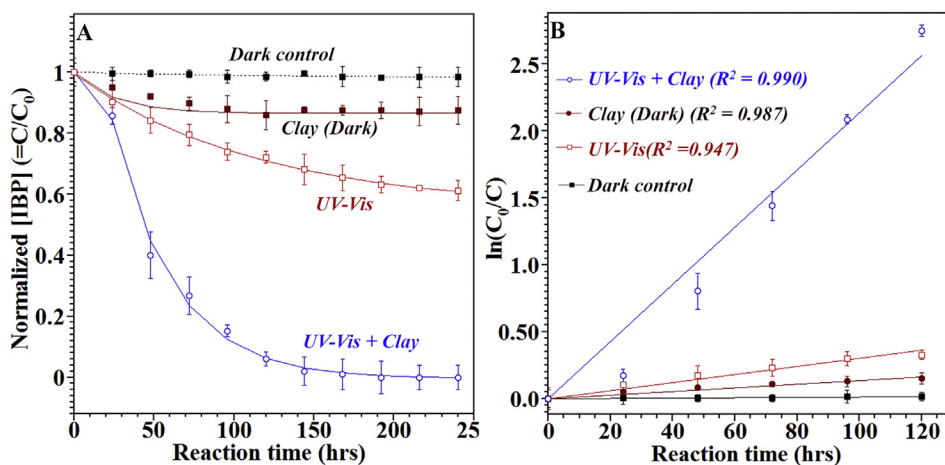
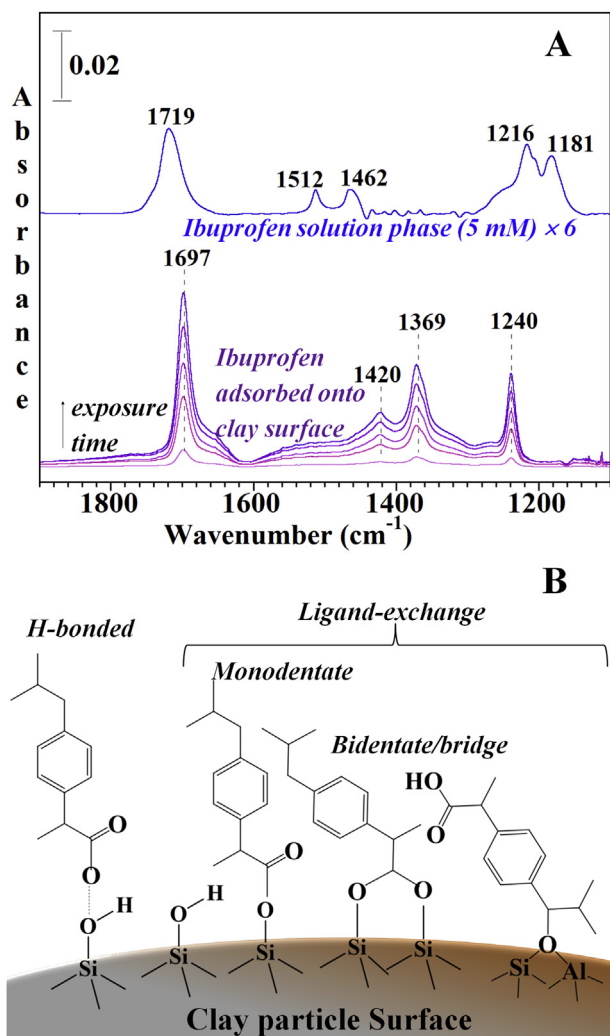


Fig. 2. A comparison of kinetics of ibuprofen decay under various experimental conditions, determined from HPLC analysis of remaining ibuprofen in degraded mixtures. A. Decay curves for ibuprofen.  $C_0$  – initial ibuprofen concentration;  $C$  – ibuprofen concentration at reaction time  $t$ . B. pseudo-first order kinetics for ibuprofen decay.  $R^2$  – correlation coefficient.

**Table 1**  
Kinetics of ibuprofen decay under various experimental conditions; decay rates ( $r$ ), mass normalized decay rates ( $r_{MN}$ ); surface area normalized decay rate, ( $r_{SAN}$ ); pseudo-first order rate constants ( $k$ ) and correlation coefficients ( $R^2$ ).

| Experimental condition | $r$ ( $10^{-4}$ M h $^{-1}$ ) | $r_{MN}$ ( $10^{-4}$ M h $^{-1}$ g $^{-1}$ ) | $r_{SAN}$ ( $10^{-4}$ M h $^{-1}$ m $^{-2}$ ) | $k$ (h $^{-1}$ )      | $R^2$ |
|------------------------|-------------------------------|--|---|-----------------------|-------|
| Dark control           | No degradation                | NR   | NR  | NR                    | NR    |
| Clay (dark)            | 0.24 ( $\pm 0.02$ )           | 12 ( $\pm 1$ )                               | 1.2 ( $\pm 0.1$ )                             | 0.0014 ( $\pm 0.10$ ) | 0.947 |
| UV-Vis                 | 0.34 ( $\pm 0.03$ )           | NR   | NR  | 0.0030 ( $\pm 0.10$ ) | 0.987 |
| UV-Vis + Clay          | 1.4 ( $\pm 0.1$ )             | 70 ( $\pm 5$ )                               | 6.9 ( $\pm 0.5$ )                             | 0.021 ( $\pm 0.001$ ) | 0.990 |

NR – Not relevant.



**Fig. 3.** Adsorption of ibuprofen on clay (kaolinite) particle surface. **A.** ATR-FTIR spectra of ibuprofen adsorption. Spectra are shown for exposure of clay to 1 mM ibuprofen for 45 min. The solution phase spectrum collected in the absence of clay is shown as well. **B.** Proposed mechanism of adsorption of ibuprofen on kaolinite surface.

### 3.2.2. Role of sunlight

The results shown in Fig. 2 clearly demonstrate that the degradation of ibuprofen is influenced by solar radiation. The initial rate of ibuprofen degradation, in the presence of only simulated sunlight (UV-Vis), is  $0.34 (\pm 0.03) \times 10^{-4}$  M h $^{-1}$ . During the period of 240 h, ~38% of initial ibuprofen was degraded. Previous studies have highlighted photodegradation of ibuprofen via hydroxyl radicals (\*OH) (Iovino et al., 2016; Matamoros et al., 2008). In the presence of a photocatalyst, e.g. TiO<sub>2</sub>, production of \*OH is enhanced by electron/hole pairs formed on the catalyst surface. (Georgaki et al., 2014). Without a catalyst, \*OH radicals are directly

produced by H<sub>2</sub>O homolysis promoted by UV light ( $\lambda < 185$  nm) (Iovino et al., 2016). Under the experimental conditions of the current work, the intensity of UV-C radiation of the simulated sunlight is expected to be low, a more environmentally relevant condition. Thus, the lower yield of \*OH radicals by H<sub>2</sub>O homolysis can partially account for the observed lower extent and degradation rates of ibuprofen compared to previous work. However, several recent studies have implicated the photodegradation of ibuprofen via self-sensitization (Li et al., 2015). Here, ibuprofen (IBP) transforms into excited ibuprofen (IBP\*) subsequent to absorbing photons ( $\lambda < 240$  nm;  $\lambda_{max} = 222$  nm), which then transfers its energy to dissolved oxygen or other oxygen rich species in the solution to generate reactive oxygen species (ROS), i.e. \*OH, H<sub>2</sub>O<sub>2</sub>. ROS subsequently causes the photooxidation of ibuprofen. Even though these mechanisms contribute to the observed photodegradation, poor overlap of emission spectrum of the simulated sunlight and absorption spectrum of free ibuprofen in solution may have yielded slower degradation rates.

As seen in Fig. 2, the photodegradation of ibuprofen is significantly enhanced in the presence of clay particles. The initial rate of degradation is  $1.40 (\pm 0.1) \times 10^{-4}$  M h $^{-1}$  which is 4-fold higher compared to that in the absence of clay particles. We observed 100% photodegradation within a period of 120 h. Further, the decay rate of ibuprofen in the presence of clay surface is at least 6-fold higher for the irradiated sample compared to that of dark conditions. Here, we propose that the observed enhancement in photodegradation is due to the adsorption of ibuprofen onto clay particle surfaces. As discussed earlier, the irreversible uptake of ibuprofen results bathochromic shifts in  $\pi$  to  $\pi^*$  and  $n$  to  $\pi^*$  transitions. These chemical shifts enhance the overlap of absorption bands of ibuprofen and emission profile of sunlight resulting higher quantum yields to produce more excited IBP\* and ROS. Thus, the surface adsorption of ibuprofen onto clay surface enhances the rate and extent of photodegradation. Several other studies on photodegradation have further proposed that the observed enhancement could be due to the generation of hydroxyl radicals from water, adsorbed on kaolinite surface (Ahn et al., 2006). Given that the rates of surface-catalyzed reactions may depend on the mass and the available surface area of the adsorbent (Georgaki et al., 2014), both mass normalized and surface area normalized degradation rates are given in Table 1. The mass normalized degradation rate,  $70 (\pm 5) \times 10^{-4}$  M h $^{-1}$  g $^{-1}$  is at least an order of magnitude higher compared to the rates reported by Madhavan et al. ( $5 \times 10^{-4}$  M h $^{-1}$  g $^{-1}$ ) where the degradation was carried out via sonophotocatalytic mechanism (Madhavan et al., 2010). However, authors further discuss that the degradation rate increases with an increase of initial concentration. Thus, the enhanced rates in the current study may be partly due to higher initial concentration of ibuprofen.

### 3.2.3. Formation of secondary products and possible reaction pathways

Formation of secondary products, as a result of ibuprofen degradation in the presence of clay particles and simulated sunlight, is shown in Fig. 4. HPLC chromatograms given in Fig. 4A

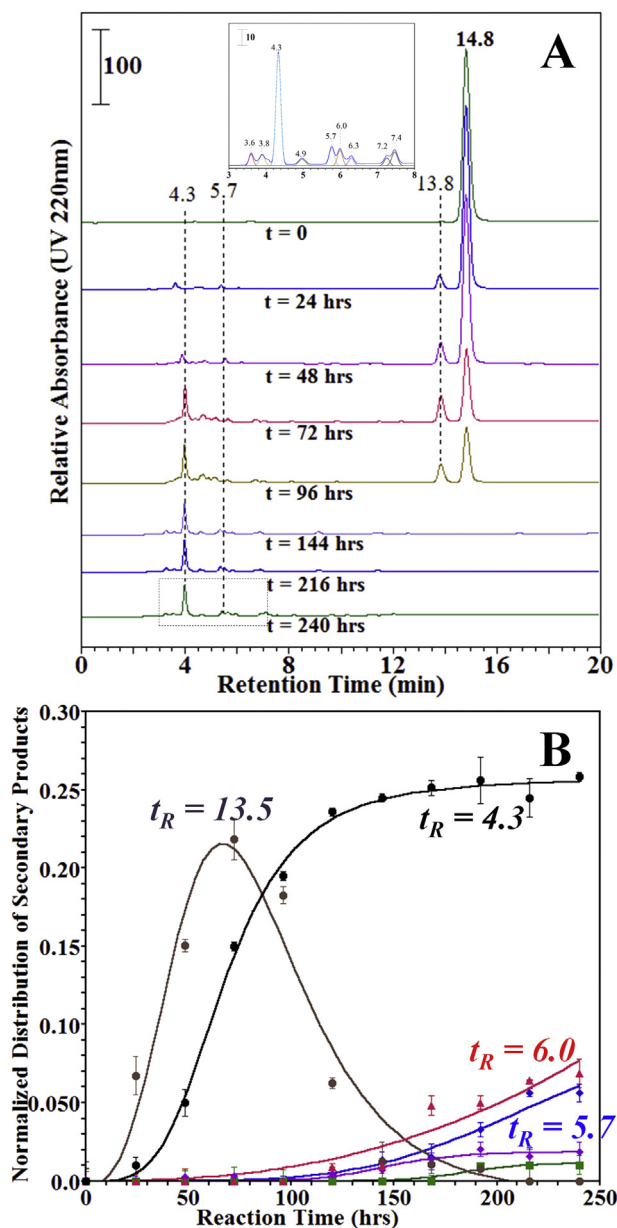


**Fig. 4.** Formation of secondary products as a result of ibuprofen degradation in the presence of clay particles and simulated sunlight. **A.** Reversed phase HPLC showing degradation of ibuprofen ( $t_R = 14.8$ ) and formation of secondary products in the presence of clay and simulated sunlight. Insert: the zoomed region within the dashed line for  $t = 240$  h. **B.** Variation of relative amounts of secondary products as a function of reaction time.

showed several new peaks in addition to the peak corresponding to ibuprofen ( $t_R = 14.8$ ). The change of relative amounts of these species as a function of reaction time is shown in Fig. 4B. Several secondary products, indicated by peaks at  $t_R = 4.3$ , 6.0, 5.7, etc., increase with reaction time where the product at  $t_R = 4.3$  is the major species towards the end of the reaction period. This was later identified as 4-acetylbenzoic acid in LC-MS studies and conformed using relative retention time of the reference material. Further, several reaction intermediates can be identified, i.e.  $t_R = 13.5$ , 3.6, based on their formation and consumption as a function of reaction time.

Liquid chromatography coupled with mass spectroscopy (LC-MS) was performed to identify these secondary products. The LC-

MS chromatogram for the fully degraded sample, after 240 h of irradiation, is shown in Fig. 5 along with respective retention times (black) and  $m/z$  values (red). Under the same LC-MS conditions, the stock solution showed a peak at 8.13 min for ibuprofen which is absent in the degraded mixture. Here, 4-acetylbenzoic acid ( $t_R = 1.93$ ;  $m/z = 164$ ) was again identified as the major degradation compound, followed by 4-(1-carboxyethyl)benzoic acid ( $t_R = 4.98$ ;  $m/z = 194$ ). The details of identified major secondary residues are given in Table 2. Many of these secondary products have previously been confirmed as degradation products of ibuprofen in both direct photolysis and surface-catalyzed photodegradation (Ding et al., 2017; Illés et al., 2013; Loaiza-Ambuludi et al., 2013; Sabri et al., 2012). However, little is known about the details of these reaction mechanisms. In the current study, three possible reaction pathways are proposed based on the identified secondary products and their variations during the reaction time. These reaction pathways are illustrated in Fig. 6. As discussed above, free ibuprofen molecule (1) is adsorbed from the aqueous medium onto the clay surface (2), and shifts its absorption profile ( $\lambda_{max}$ ) to lower wavenumbers. Upon exposure to solar radiation, the surface adsorption complex (2) is transformed into excited ibuprofen (3) that undergoes direct and indirect degradation. The photodegradation pathways described in this study involves hydroxylation ( $^*OH$ ), decarboxylation ( $-CO_2$ ), and demethylation ( $-CH_3$ ). One such possible route is shown by intermediates and products from (4) through (7). Here, the attack of  $^*OH$  on isobutyl substituent of adsorbed IBP structure that results in subsequent oxidation. In similar studies, Li et al. among several others, also report that the hydroxylation of the benzylic carbon could be the first step of ibuprofen degradation (Li et al., 2014; Madhavan et al., 2010; Méndez-Arriaga et al., 2010).

In the second possible route,  $^*OH$  attacks the benzyl carbon of the carboxylic acid residue of the adsorbed ibuprofen (3) to yield a hydroxylated compound (8) which is transformed to 4-acetylbenzoic acid (14), the most abundant secondary residue observed in this study. We propose that this transformation occurs via a second hydroxylation at the benzyl carbon on the isobutyl residue of the ketone (10) to form (11) which may oxidize to isobutyrylbenzoic acid (12). Though we did not observe (11) and (12) in our LC-MS analysis, Xiang et al., confirms the formation of hydroxylated benzyl ketone (11) in a similar study. Demethylation of compound (13) via retro-aldol or a similar mechanism will yield (14). In several other studies, it has also shown that oxidation of ketone group in compound (10) can occur prior to hydroxylation and form 4-isobutylbenzoic acid (15) (Caviglioli et al., 2002).

In LC-MS analysis, we observed several secondary residues with higher  $m/z$  values, i.e. 248, 252, 275. The proposed structure for  $m/z = 248$  is shown as compound (16). Products with such higher  $m/z$  values have been observed in other ibuprofen degradation studies (Illés et al., 2013). It is postulated that multi-hydroxylation may initiate free-radical reactions that could potentially grow the side chains to result secondary residues with higher  $m/z$  values. However, it should be mentioned that future studies should be carried out on these secondary residues to further confirm their structures and formation mechanisms.

### 3.3. Toxicological studies

Toxicity of ibuprofen and its secondary residues were assessed on two bacterial species, *Bacillus megaterium* and *Pseudoaltermonas atlantica*, and one green algae, *Chlorella* sp. It should be pointed out that these toxicological studies were mainly focused on evaluating relative health effects of primary IBP and its degraded products. In this study, growth rates and viability were measured using OD

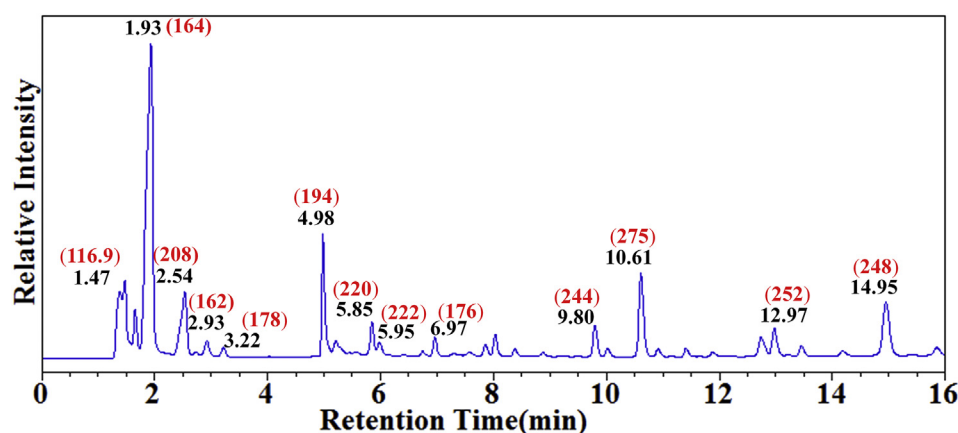


**Fig. 5.** LC-MS analysis of secondary products of ibuprofen yielded from abiotic degradation in the presence of kaolinite upon irradiation. Given relation times (black) and m/z value (red). (For interpretation of the references to colour in this figure legend, the reader is referred to the Web version of this article.)

**Table 2**  
IUPAC name, HPLC retention time, and molecular weight of ibuprofen degradation products.

| Id # | IUPAC name  | Retention time ( $t_R$ ) (min) | Molecular weight ( $\text{g mol}^{-1}$ ) | Ref.  |
|------|---|--------------------------------|--|---|
| (4)  | 2-(4-(1-hydroxyisobutyl)phenyl)propanoic acid     | 5.95                           | 222                                      | (Caviglioli et al., 2002; Li et al., 2014; Méndez-Arriaga et al., 2010)           |
| (5)  | 2-(4-isobutrylphenyl)propanoic acid               | 5.85                           | 220                                      | (Li et al., 2014; Persson Stubberud and Åström, 1998)                             |
| (6)  | 2-(4-formylphenyl)propanoic acid                  | 3.22                           | 178                                      | (Caviglioli et al., 2002; Illés et al., 2013)                                     |
| (7)  | 4-(1-carboxyethyl)benzoic acid                    | 3.22                           | 194                                      | (Caviglioli et al., 2002; Madhavan et al., 2010)                                  |
| (8)  | 2-hydroxy-2-(4-isobutylphenyl)propanoic acid      | 5.95                           | 222                                      | (Li et al., 2014; Méndez-Arriaga et al., 2008)                                    |
| (9)  | 1-(4-isobutylphenyl)ethan-1-ol                    | 3.22                           | 178                                      | (Jacobs et al., 2011; Loaiza-Ambuludi et al., 2013; Skoumal et al., 2009)         |
| (10) | 1-(4-isobutylphenyl)ethan-1-one                   | 6.87                           | 176                                      | (Loaiza-Ambuludi et al., 2013; Méndez-Arriaga et al., 2010; Skoumal et al., 2009) |
| (11) | 1-(4-(1-hydroxy-2-methylpropyl)phenyl)ethan-1-one | n.o.                           | 192                                      | (Li et al., 2014)   |
| (12) | 4-isobutrylbenzoic acid                           | n.o.                           | 192                                      |   |
| (13) | 4-(3-hydroxy-2-methylpropanoyl)benzoic acid       | 2.54                           | 208                                      | (Ding et al., 2017; Méndez-Arriaga et al., 2008)                                  |
| (14) | 4-acetylbenzoic acid                              | 1.93                           | 164                                      | (Caviglioli et al., 2002; Sabri et al., 2012)                                     |
| (15) | 4-isobutylbenzoic acid                            | 3.20                           | 178                                      | (Caviglioli et al., 2002; Illés et al., 2013)                                     |
| (16) | 2-(4-isobutylphenyl)-5-methylhexan-3-ol           | 14.95                          | 248                                      | (Illés et al., 2013)  |

n.o. – not observed in the current study.

measurements, MTT assay, and flow cytometry. Results for MTT assay were normalized using both the negative (non-treated) and PAO-killed control. Absorbance signals from the non-treated or PAO treated cells were considered to be 100% viable or 100% dead, respectively and used as a reference to calculate and compare the % growth of bacteria undergoing treatment.

### 3.3.1. Growth inhibition of *B. megaterium* and *P. atlantica*

At high concentrations, exposure to primary PPCP, ibuprofen, resulted in significant reduction of viability of *B. megaterium* and *P. atlantica*. In contrast, treatment of both bacterial cells with a mixture of degraded secondary products, generated from the same initial ibuprofen concentration, had little impact on their viability. The results of MTT viability assay are shown in Fig. 7. Less than 50% of the *B. megaterium* cells were viable after 1 mM ibuprofen treatment for 48 h (Fig. 7A). Similarly, the viability of *P. atlantica* was reduced to about 80% when treated with 1 mM of ibuprofen (Fig. 7B). However, at 0.5 mM viability decreased significantly for *B. megaterium* ( $p = 0.007$ ) whereas *P. atlantica* remained unaffected ( $p = 0.106$ ). Conversely, exposure of *B. megaterium* and *P. atlantica* to a mixture of secondary products produced little to no effect on viability of either of these bacterial species. Although toxicity of phototransformed PPCP mixtures has been rarely studied, few

studies have suggested synergistic or antagonistic effects due to pharmacokinetic interactions (Celander, 2011). Interestingly, exposure to the mixture of secondary residues, at a total concentration of 1 mM, demonstrated a slight promotion of both *B. megaterium* ( $p = 0.031$ ) and *P. atlantica* ( $p = 0.038$ ) growth. No inhibition or enhancement was observed for any lower concentrations of the secondary product mixture. This could be due to a biological phenomenon called 'hormesis' which represents a biphasic dose response, promoting growth during mild chemical stress or low concentrations (Hashmi et al., 2014). Since secondary product mixture is a combination of a number of phototransformed products, concentration of individual secondary residues in the mixture is much lower than that of the original primary compound (ibuprofen). Thus, the mixture of secondary residues might actually exhibit low-dose bacterial growth stimulation. Additional biological assays were carried out using 4-acetylbenzoic acid, the most abundant secondary residue. No significant toxic effect was observed on either of the bacterial species. Nevertheless, *B. megaterium*, exposed to 1 mM ( $p = 0.007$ ) and 0.5 mM ( $p = 0.027$ ) of 4-acetylbenzoic acid, showed a small promotion of growth. Toxic effects of ibuprofen and its secondary products were further confirmed with growth rate analysis of both these species using OD measurements (SI Fig. 2).

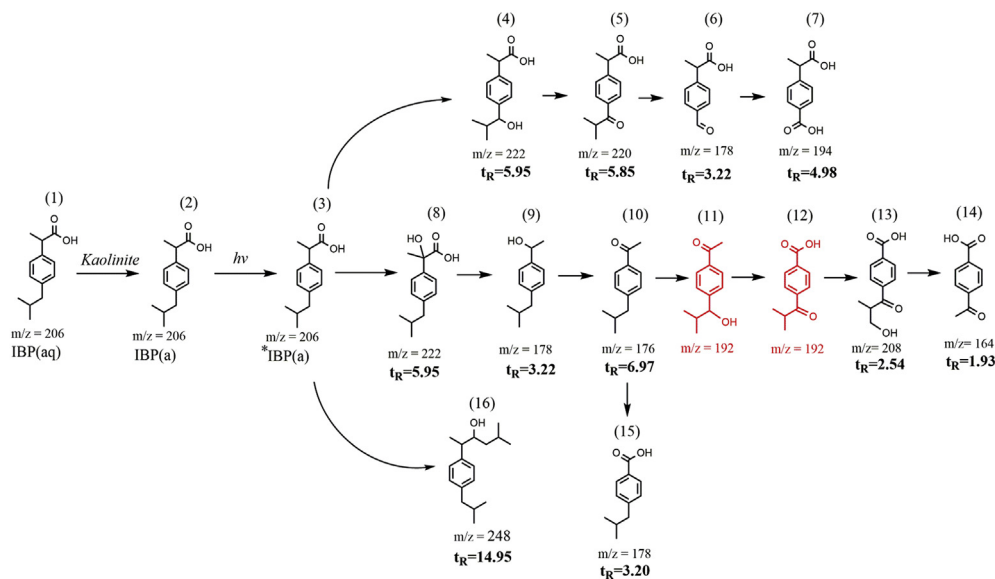


**Fig. 6.** Proposed reaction mechanism for the abiotic degradation of ibuprofen in the presence of kaolinite and sunlight. Intermediates and products observed in the current work are shown in black whereas the proposed intermediates are shown in red. (For interpretation of the references to colour in this figure legend, the reader is referred to the Web version of this article.)

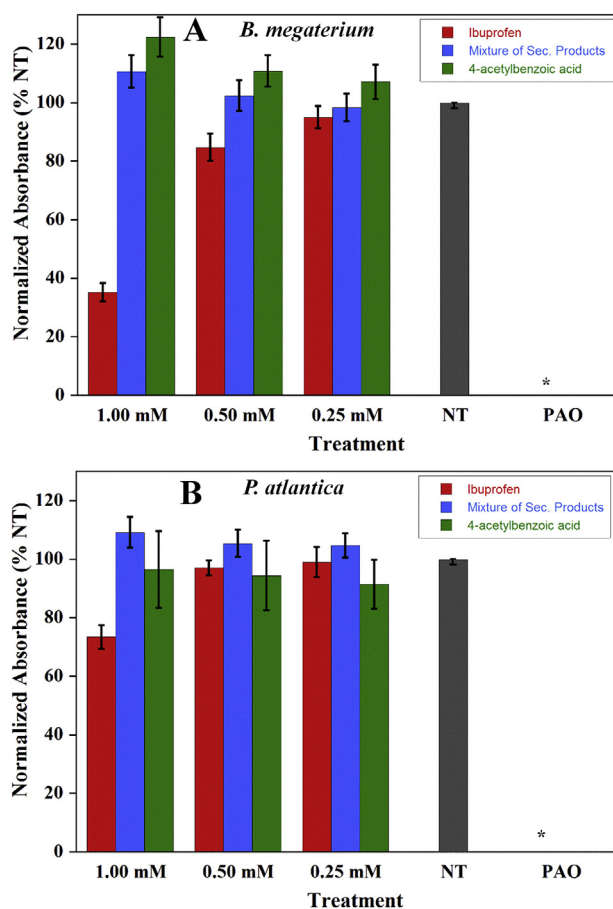


**Fig. 7.** MTT assay for bacteria after 24 h of exposure to ibuprofen, its secondary products mixtures and 4-acetylbenzoic acid. **A.** *B. megaterium*, and **B.** *P. atlantica*. (\* – 100% kill or '0' absorbance).

The antibacterial property of ibuprofen has been previously discussed in several recent studies (Al-Janabi, 2010; Farre et al.,

2001; Obad et al., 2015). Farre et al. have reported the toxicity of ibuprofen on *Vibrio fischeri* with  $EC_{50}$  values of 12.1  $\mu\text{g}/\text{mL}$  in ToxAlert 100<sup>®</sup> assay and 19.1  $\mu\text{g}/\text{mL}$  in Microtox<sup>®</sup> assay. The mode of toxicological action of NSAIDs on bacteria is not fully understood. However, it has been suggested that the mode of action is similar to that on fungi (Al-Janabi, 2010). In an earlier study, it has been further shown that exposure of *Candida albicans* to ibuprofen at a concentration of 10  $\text{mg}/\text{mL}$  results in complete dissolution of its cytoplasmic membrane (Pina-Vaz et al., 2000). The non-toxic effect of secondary product mixture on bacteria can be attributed to the degradation of ibuprofen to the less toxic secondary residues. It can also be argued that the presence of various secondary products might give rise to an antagonistic effect which could result in no observable toxicity effect. However, the near-absence of bacterial toxicity upon treatment to 4-acetylbenzoic acid supports the hypothesis of formation of significantly lesser toxic products.

### 3.3.2. Growth inhibition of *Chlorella* sp.

Given that Chlorophyll *a* autofluorescence is a measure of algal photosynthetic activity, change in the intrinsic fluorescence of the freshwater green algae was used as the indicator of ibuprofen toxicity. Since chlorophyll *a* fluorescence is usually a measure of photosystem II (PSII) activity, the significant reduction in the FL3 signal can be attributed to the inactivation of PSII reaction centers. In the current study, algae samples were excited at ~488 nm and the fluorescence emission was determined in the red channel (FL3, ~670 nm) of the FACSCalibur flow cytometer. Fluorescence scatter plots (insets in Fig. 8A–D) were used to generate histogram plots consisting two regions of interest R1, and R2. These two regions represent negative shift (inhibition of algae growth) and control region (normal growth), respectively. Histograms of non-treated and treated algae samples after 48 h of exposure are shown in Fig. 8A–D. Number of algal cells in R1 region has increased and the number of cells in R2 region has decreased for 1 mM ibuprofen and 1 mM 4-acetylbenzoic acid treatments, indicating a significant effect on algal growth. In contrast, 1 mM secondary products have a comparable to that of untreated control sample indicating no significant effect on algal growth. Quantitative analysis of Fig. 8E was conducted according to the following equation:

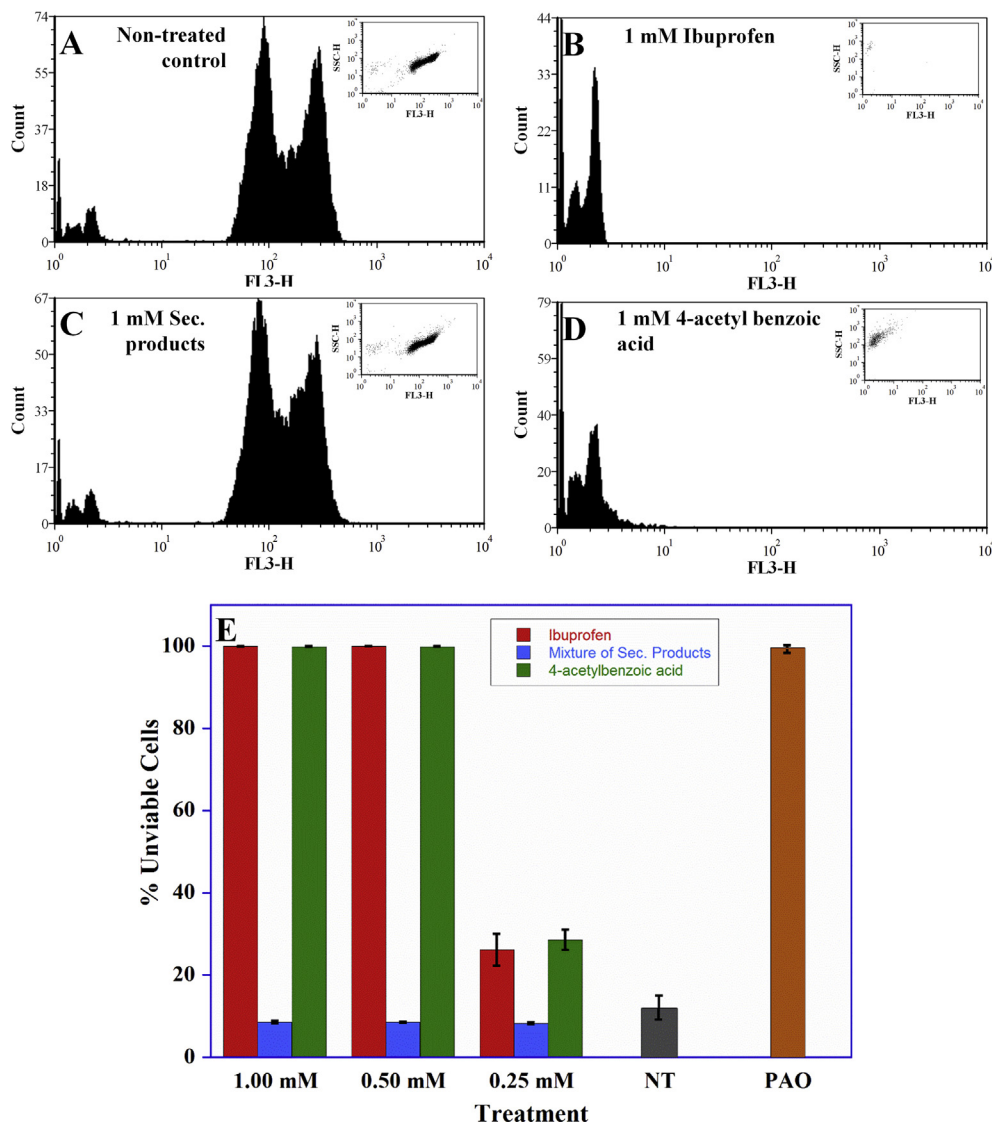


**Fig. 8.** Flow cytometry assay for *Chlorella* sp. to evaluate the effect of ibuprofen, mixture of its secondary products, and 4-acetylbenzoic acid on chlorophyll after 48 h of exposure **A–D.** Fluorescence histograms of untreated and treated algae samples generated from fluorescence scatter plots (insets). **E.** Comparison of toxicity for various concentrations of ibuprofen, its secondary products, and 4-acetylbenzoic acid.

$$\% \text{ Nonviable cells} = \frac{\text{Number of counts in region R1}}{\text{Total number of counts}} \times 100 \quad (1)$$

Exposure to ibuprofen at 0.5 mM or higher resulted in almost 100% dead cells while little or no toxicity was observed for the secondary mixture at all concentrations studied. 1 mM secondary product mixture-treatment of alga results no significant toxicity ( $p = 0.374$ ) compared to the control. More interestingly, 4-acetylbenzoic acid showed significant toxic effects even at lower concentrations and nearly the entire algal population was killed at concentrations higher than 0.5 mM. Similar ibuprofen toxicity has been reported by Moro et al. who investigated the effect of ibuprofen on *Scenedesmus rubescens*, a freshwater green microalga (Moro et al., 2014). Algal cells demonstrated a growth inhibition and reduction in chlorophyll content upon exposure to 1 mg/L of ibuprofen (Geiger et al., 2016). In a related study, Jiao et al. reported growth inhibition among *Chlorella vulgaris* by 0.5 mg/L of ethyl

cinnamate, a commonly used flavor ingredient (Jiao et al., 2015). This study further revealed that ethyl cinnamate induces a photosynthetic toxic which significantly affect the chlorophyll fluorescence.

As for bacteria, a decrease in toxicity would indeed due to degradation to less toxic – and less abundant – products. Indeed, the variation in the effect posed by ibuprofen and its secondary products can arise from the formation of significantly less toxic metabolites. However, the significant toxicity due to single treatment of 4-acetylbenzoic acid could be due to the presence of the compound in high concentration compared to its relative low concentration when present in the mixture. Another possibility could be the significant difference in  $pK_a$  between the primary compound and its degraded products. Ibuprofen has higher reported  $pK_a$  value of 5.2 (Meloun et al., 2007) whereas 4-acetylbenzoic acid has a  $pK_a$  value of 3.7 (Dewick, 2006). Thus, based on the pH of the growth medium, the distribution of neutral (acid) and anionic forms of ibuprofen and 4-actylebenzoic acid could show significant differences. These variations can have a

considerable impact in their toxic effects. Earlier studies conducted by Franklin et al. (2000) and Wilde et al. (2006) among others have also confirmed that toxicity in *Chlorella* is highly pH-dependent.

#### 4. Conclusions

This study investigated abiotic degradation pathways of ibuprofen, an abundant PPCP, in the presence of clay particles, via chemical and photochemical reaction pathways. In the absence of solar radiation the dominant reaction mechanism was observed to be the heterogeneous uptake of ibuprofen on to clay surface via surface silanol groups to form monodentate and bidentate modes of coordination. In contrast, upon irradiation, ibuprofen breaks down to several fractions via clay-catalyzed photoreactions. The decay rates were at least 6-fold higher for irradiated samples compared to that of dark conditions. The enhanced degradation rates and extent, in presence of clay and solar radiation, can be attributed to the bathochromic shift of absorption bands by the adsorbed ibuprofen. Here, several reaction pathways were proposed for the abiotic degradation of ibuprofen, via direct and self-sensitized mechanisms, that involves hydroxylation, decarboxylation, and demethylation. The current study also evaluates the relative toxic effects of primary ibuprofen and its secondary residues. Ibuprofen-induced toxicity was far more significant than the toxicity of its secondary/degraded products in all the three test organisms used in this study. In general, ibuprofen resulted in the reduction of growth/survival rate and autofluorescence. In contrast, the degraded products resulted in little to no toxicity effect in all three organisms. However, varied degree of toxicity was observed among the test organisms when exposed to high concentrations of 4-acetylbenzoic acid, the most abundant secondary compound formed in the mixture upon irradiation.

PPCPs are considered to be a potential threat to the environment as well as human health due to their potential accumulation and magnification in aquatic systems. Several groups of PPCPs, i.e. disinfectants, have been approved to be able to bioaccumulate and probably biomagnify and may finally cause adverse effects to human beings. Our current work clearly shows, not only via food web but also on mineral particles, PhAC such as ibuprofen accumulate with aquatic systems. Based on our findings and several others, one could argue that, in the past PPCP field and laboratory studies, “we have been looking for the wrong thing at the wrong place”. The reason is that we have been trying to quantify primary PPCP compounds not knowing they degrade at higher rate in the environmental time scale. And, if these PPCPs and secondary residues partition into clay and sediments, then we were looking at the wrong place. Thus, the current study advances our knowledge and understanding in the fields of environmental toxicology, chemistry in aqueous phases, and geochemistry.

#### Funding

This work was supported by an Institutional Development Award (IDeA) from the National Institute of General Medical Sciences of the National Institutes of Health (P20GM103451).

#### Acknowledgment

We would like to acknowledge Prof. Rodolfo Tello-Aburto (New Mexico Tech) for helpful discussions on organic reaction mechanisms and Dr. Tanner Schaub (New Mexico State University) for technical assistance with LC-MS studies. And authors would like to thank Eshani Hettiarachchi for her support in SEM imaging and XRD experiments.

#### Appendix A. Supplementary data

Supplementary data related to this article can be found at <https://doi.org/10.1016/j.watres.2017.12.016>.

#### References

- Aceña, J., Pérez, S., Eichhorn, P., Solé, M., Barceló, D., 2017. Metabolite profiling of carbamazepine and ibuprofen in solea senegalensis bile using high-resolution mass spectrometry. *Anal. Bioanal. Chem.* 409 (23), 5441–5450.
- Ahn, M.-Y., Filley, T.R., Jafvert, C.T., Nies, L., Hua, L., Bezares-Cruz, J., 2006. Photodegradation of decarbomodiphenyl ether adsorbed onto clay minerals, metal oxides, and sediment. *Environ. Sci. Technol.* 40 (1), 215–220.
- Al-Janabi, A.A., 2010. In vitro antibacterial activity of ibuprofen and acetaminophen. *J. Global Infect. Dis.* 2 (2), 105–108.
- Blair, B.D., Crago, J.P., Hedman, C.J., Klaper, R.D., 2013. Pharmaceuticals and personal care products found in the great lakes above concentrations of environmental concern. *Chemosphere* 93 (9), 2116–2123.
- Blasco, T., 2010. Insights into reaction mechanisms in heterogeneous catalysis revealed by in situ NMR spectroscopy. *Chem. Soc. Rev.* 39 (12), 4685–4702.
- Boxall, A.B.A., Rudd, M.A., Brooks, B.W., Caldwell, D.J., Choi, K., Hickmann, S., Innes, E., Ostapyk, K., Staveley, J.P., Verslycke, T., Ankley, G.T., Beazley, K.F., Belanger, S.E., Berninger, J.P., Carriquiriborde, P., Coors, A., DeLeo, P.C., Dyer, S.D., Ericson, J.F., Gagne, F., Giesy, J.P., Gouin, T., Hallstrom, L., Karlsson, M.V., Larsson, D.G.J., Lazorchak, J.M., Mastrocco, F., McLaughlin, A., McMaster, M.E., Meyerhoff, R.D., Moore, R., Parrott, J.L., Snape, J.R., Murray-Smith, R., Servos, M.R., Sibley, P.K., Straub, J.O., Szabo, N.D., Topp, E., Tetreault, G.R., Trudeau, V.L., Van Der Kraak, G., 2012. Pharmaceuticals and personal care products in the environment: what are the big questions? *Environ. Health Perspect.* 120 (9), 1221–1229.
- Caviglioli, G., Valeria, P., Brunella, P., Sergio, C., Attilia, A., Gaetano, B., 2002. Identification of degradation products of ibuprofen arising from oxidative and thermal treatments. *J. Pharmaceut. Biomed. Anal.* 30 (3), 499–509.
- Celander, M.C., 2011. Cocktail effects on biomarker responses in fish. *Aquat. Toxicol.* 105, 72–77.
- Deo, R., 2014. Pharmaceuticals in the surface water of the USA: a review. *Curr. Environ. Health Rpt.* 1 (2), 113–122.
- Dewick, P.M., 2006. *Essentials of Organic Chemistry: For Students of Pharmacy, Medicinal Chemistry and Biological Chemistry*. John Wiley & Sons, Ltd.
- Ding, T., Yang, M., Zhang, J., Yang, B., Lin, K., Li, J., Gan, J., 2017. Toxicity, degradation and metabolic fate of ibuprofen on freshwater diatom *Navicula* sp. *J. Hazard Mater.* 330, 127–134.
- Farre, M.L., Ferrer, I., Ginebreda, A., Figueras, M., Olivella, L., Tirapu, L., Vilanova, M., Barcelo, D., 2001. Determination of drugs in surface water and wastewater samples by liquid chromatography-mass spectrometry: methods and preliminary results including toxicity studies with *vibrio fischeri*. *J. Chromatogr. A* 938 (1–2), 187–197.
- Franklin, N.M., Stauber, J.L., Markich, S.J., Lim, R.P., 2000. Ph-dependent toxicity of copper and uranium to a tropical freshwater alga (*Chlorella* sp.). *Aquat. Toxicol.* 48 (2–3), 275–289.
- Geiger, E., Hornek-Gausterer, R., Sacan, M.T., 2016. Single and mixture toxicity of pharmaceuticals and chlorophenols to freshwater algae *Chlorella vulgaris*. *Ecotoxicol. Environ. Saf.* 129, 189–198.
- Georgaki, I., Vasilaki, E., Katsarakis, N., 2014. A study on the degradation of carbamazepine and ibuprofen by TiO<sub>2</sub> & ZnO photocatalysis upon UV/visible-light irradiation. *Am. J. Anal. Chem.* 5 (8), 518–534.
- Hashmi, M.Z., Naveedullah, Shen, H., Zhu, S.H., Yu, C.N., Shen, C.F., 2014. Growth, bioluminescence and shoal behavior hormetic responses to inorganic and/or organic chemicals: a review. *Environ. Int.* 64, 28–39.
- Illés, E., Takács, E., Dombi, A., Gajda-Schrantz, K., Rácz, G., Gonter, K., Wojnárovits, L., 2013. Hydroxyl radical induced degradation of ibuprofen. *Sci. Total Environ.* 447, 286–292.
- Iovino, P., Chianese, S., Canzano, S., Prisciandaro, M., Musmarra, D., 2016. Degradation of ibuprofen in aqueous solution with UV light: the effect of reactor volume and pH. *Water Air Soil Pollut.* 227 (6), 194.
- Jacobs, L.E., Fimmen, R.L., Chin, Y.-P., Mash, H.E., Weavers, L.K., 2011. Fulvic acid mediated photolysis of ibuprofen in water. *Water Res.* 45 (15), 4449–4458.
- Jiao, Y., Ouyang, H.L., Jiang, Y.J., Kong, X.Z., He, W., Liu, W.X., Yang, B., Xu, F.L., 2015. Toxic effects of ethyl cinnamate on the photosynthesis and physiological characteristics of *Chlorella vulgaris* based on chlorophyll fluorescence and flow cytometry analysis. *Sci. World J.* 2015, 107823.
- Kamarudin, N.H.N., Jalil, A.A., Triwahyono, S., Sazegar, M.R., Hamdan, S., Baba, S., Ahmad, A., 2015. Elucidation of acid strength effect on ibuprofen adsorption and release by aluminated mesoporous silica nanoparticles. *RSC Adv.* 5 (38), 30023–30031.
- Khan, U., Nicell, J., 2015. Human health relevance of pharmaceutically active compounds in drinking water. *AAPS J.* 17 (3), 558–585.
- Khazri, H., Ghorbel-Abid, I., Kalfat, R., Trabelsi-Ayadi, M., 2016. Removal of ibuprofen, naproxen and carbamazepine in aqueous solution onto natural clay: equilibrium, kinetics, and thermodynamic study. *Appl. Water Sci.* 1–10.
- Kolpin, D.W., Furlong, E.T., Meyer, M.T., Thurman, E.M., Zaugg, S.D., Barber, L.B., Buxton, H.T., 2002. Pharmaceuticals, hormones, and other organic wastewater contaminants in us streams, 1999–2000: a national reconnaissance. *Environ. Sci.*

- Technol. 36 (6), 1202–1211.
- Kortenkamp, A., Backhaus, T., Faust, M., 2009. State of the Art Report on Mixture Toxicity. European Commission, Brussels, Belgium.
- Li, F.H., Yao, K., Lv, W.Y., Liu, G.G., Chen, P., Huang, H.P., Kang, Y.P., 2015. Photodegradation of ibuprofen under UV–vis irradiation: mechanism and toxicity of photolysis products. *Bull. Environ. Contam. Toxicol.* 94 (4), 479–483.
- Li, W.C., 2014. Occurrence, sources, and fate of pharmaceuticals in aquatic environment and soil. *Environ. Pollut.* 187, 193–201.
- Li, X., Wang, Y., Yuan, S., Li, Z., Wang, B., Huang, J., Deng, S., Yu, G., 2014. Degradation of the anti-inflammatory drug ibuprofen by electro-peroxone process. *Water Res.* 63, 81–93.
- Loaiza-Ambuludi, S., Panizza, M., Oturan, N., Özcan, A., Oturan, M.A., 2013. Electro-fenton degradation of anti-inflammatory drug ibuprofen in hydroorganic medium. *J. Electroanal. Chem.* 702, 31–36.
- Madhavan, J., Grieser, F., Ashokkumar, M., 2010. Combined advanced oxidation processes for the synergistic degradation of ibuprofen in aqueous environments. *J. Hazard Mater.* 178 (1–3), 202–208.
- Madieh, S., Simone, M., Wilson, W., Mehra, D., Augsburger, L., 2007. Investigation of drug–porous adsorbent interactions in drug mixtures with selected porous adsorbents. *J. Pharm. Sci.* 96 (4), 851–863.
- Matamoros, V., Duhec, A., Albaigés, J., Bayona, J.M., 2008. Photodegradation of carbamazepine, ibuprofen, ketoprofen and 17 $\alpha$ -ethinylestradiol in fresh and seawater. *Water Air Soil Pollut.* 196 (1), 161.
- Meloun, M., Bordovska, S., Galla, L., 2007. The thermodynamic dissociation constants of four non-steroidal anti-inflammatory drugs by the least-squares nonlinear regression of multiwavelength spectrophotometric ph-titration data. *J. Pharmaceut. Biomed.* 45 (4), 552–564.
- Méndez-Arriaga, F., Esplugas, S., Giménez, J., 2008. Photocatalytic degradation of non-steroidal anti-inflammatory drugs with TiO<sub>2</sub> and simulated solar irradiation. *Water Res.* 42 (3), 585–594.
- Méndez-Arriaga, F., Esplugas, S., Giménez, J., 2010. Degradation of the emerging contaminant ibuprofen in water by photo-fenton. *Water Res.* 44 (2), 589–595.
- Moro, I., Matozzo, V., Piovan, A., Moschin, E., Vecchia, F.D., 2014. Morpho-physiological effects of ibuprofen on *scenedesmus rubescens*. *Environ. Toxicol. Pharmacol.* 38 (2), 379–387.
- Obad, J., Suskovic, J., Kos, B., 2015. Antimicrobial activity of ibuprofen: new perspectives on an "old" non-antibiotic drug. *Eur. J. Pharmaceut. Sci.* 71, 93–98.
- Overturf, M.D., Anderson, J.C., Pandelides, Z., Beyger, L., Holdway, D.A., 2015. Pharmaceuticals and personal care products: a critical review of the impacts on fish reproduction. *Crit. Rev. Toxicol.* 45 (6), 469–491.
- Persson Stubberud, K., Åström, O., 1998. Separation of ibuprofen, codeine phosphate, their degradation products and impurities by capillary electrophoresis: II. Validation. *J. Chromatogr. A* 826 (1), 95–102.
- Pina-Vaz, C., Sansonetty, F., Rodrigues, A.G., Martinez-De-Oliveira, J., Fonseca, A.F., Mardh, P.A., 2000. Antifungal activity of ibuprofen alone and in combination with fluconazole against candida species. *J. Med. Microbiol.* 49 (9), 831–840.
- Sabri, N., Hanna, K., Yargeau, V., 2012. Chemical oxidation of ibuprofen in the presence of iron species at near neutral pH. *Sci. Total Environ.* 427–428, 382–389.
- Schuttlefield, J.D., Cox, D., Grassian, V.H., 2007. An investigation of water uptake on clays minerals using ATR-FTIR spectroscopy coupled with quartz crystal microbalance measurements. *J. Geophys. Res.: Atmos.* 112 (D21).
- Siampiringue, M., Wong Wah Chung, P., Koriko, M., Tchangbedji, G., Sarakha, M., 2014. Clay and soil photolysis of the pesticides mesotrione and metsulfuron methyl. *Appl. Environ. Soil Sci.* 2014, 8.
- Skoumal, M., Rodríguez, R.M., Cabot, P.L., Centellas, F., Garrido, J.A., Arias, C., Brillas, E., 2009. Electro-fenton, uva photoelectro-fenton and solar photoelectro-fenton degradation of the drug ibuprofen in acid aqueous medium using platinum and boron-doped diamond anodes. *Electrochim. Acta* 54 (7), 2077–2085.
- Ternes, T.A., Herrmann, N., Bonerz, M., Knacker, T., Siegrist, H., Joss, A., 2004. A rapid method to measure the solid-water distribution coefficient (K<sub>d</sub>) for pharmaceuticals and musk fragrances in sewage sludge. *Water Res.* 38 (19), 4075–4084.
- Wilde, K.L., Stauber, J.L., Markich, S.J., Franklin, N.M., Brown, P.L., 2006. The effect of pH on the uptake and toxicity of copper and zinc in a tropical freshwater alga (*Chlorella* sp.). *Arch. Environ. Con. Tox.* 51 (2), 174–185.
- Xu, J., Wu, L., Chang, A.C., 2009. Degradation and adsorption of selected pharmaceuticals and personal care products (PPCPs) in agricultural soils. *Chemosphere* 77 (10), 1299–1305.